Superlattices and Microstructures 60 (2013) 240–247

Contents lists available at SciVerse ScienceDirect

Superlattices and Microstructures

journal homepage: www.elsevier.com/locate/superlattices

Tunable electron wave filter and Goos–Hänchen shift in asymmetric graphene double magnetic barrier structures

Y. Wang [a], Y. Liu [b], B. Wang [a,*]

[a] School of Physics and Engineering, Sun Yat-sen University, 510275 Guangzhou, China
[b] School of Engineering, Sun Yat-sen University, 510275 Guangzhou, China

ARTICLE INFO

Article history:
Received 23 January 2013
Received in revised form 15 April 2013
Accepted 26 April 2013
Available online 13 May 2013

Keywords:
Magnetic barrier
Transmission gap
Goos–Hänchen shift
Filter
Graphene

ABSTRACT

Electronic transmission and Goos–Hänchen shift for Dirac fermions in asymmetric graphene double magnetic barrier structure are investigated theoretically. Numerical results for rectangular barriers demonstrate that a transmission gap appears owing to the magnetic confinement and the width of gap is dependent on the incident angle and changed by the width of barrier and the distance between the double barriers. At the edge of the transmission gap, the Goos–Hänchen shifts of electrons have strong peaks and are tuned by the structure parameters. Furthermore, for the real magnetic structure induced by ferromagnetic strips, the transmission gap and GH shift remain. The tunable transmission gap indicates that the graphene magnetic structure can be use as electron wave filter and the tunable GH shift shows that the structure can be applied to laterally manipulate Dirac fermions in graphene.

1. Introduction

Since the successful fabrication of graphene, the effect of magnetic field on the transport behaviors of Dirac fermions in graphene has aroused a great deal of attention [1–4]. Recently, inhomogeneous magnetic field on submicron scales is focused on and applied to manipulate the Dirac fermions in graphene, such as magnetic confinement, anisotropic tunneling through single, double or multi magnetic barriers [5–12], the bound states of magnetic quantum dot, wire or annulus [13–20], electron

* Corresponding author. Tel.: +86 20 8411 5692; fax: +86 20 8411 3293.
E-mail address: bwang6367@gmail.com (B. Wang).

0749-6036/$ - see front matter © 2013 Elsevier Ltd. All rights reserved.
http://dx.doi.org/10.1016/j.spmi.2013.04.035

waveguide induced by magnetic barriers [17,21–24], tunneling magnetoresistance [25–27], magneto-transport and Fabry–Pérot type resonance [28–32]. Usually, the inhomogeneous magnetic field perpendicular to graphene plane is experimentally achieved by depositing ferromagnetic strips on graphene or local strain from the substrate beneath graphene [8,33].

Electron wave filter (electron wave energy filter), which forbids the electron wave at specific energy range, is one of important electronic devices. Recently, graphene-based electron wave filter has been proposed by inhomogeneous magnetic field or gate-controlled potential barrier [6,34]. However, the incident range in gate-controlled potential barrier is limited at oblique incidence due to the Klein tunneling [35]. The angular range of the transmission through graphene magnetic barrier structures can be controlled by increasing the number of magnetic barriers [6], owing to the magnetic confinement suppressing the Klein tunneling. In this present work, we consider an asymmetric graphene double magnetic barrier structure (DMBs) induced by ferromagnetic strips on graphene to design an electron wave filter based on the transmission gap occurring in this system. It is found that the width of the transmission gap can be tuned by the distance between the two barriers and the distance between ferromagnetic strip and graphene plane.

Quantum Goos–Hänchen (GH) shift is an analogy of optical GH shift, which is referred to a lateral shift between the reflected beam and the incident beam occurring at the interface of two different materials on total internal reflection [36]. It have been figured out that the reflected and transmitted Dirac fermion beams in graphene PN junction, strained barrier, magnetic barrier and velocity barrier exhibit obvious quantum GH effect [37–43], which plays an important role on the manipulation of electrons in graphene and provides an important path for achieving valley or spin splitters. In this present work, we will present the GH shift of the reflected and transmitted Dirac fermion beams in the asymmetric graphene DMBs. It is found that Dirac fermions in this structure exhibit obvious GH shifts at the edge of the transmission gap.

2. Model and theory

The graphene-based magnetic structure in Fig. 1 is designed by depositing double ferromagnetic strips on the top of an insulated oxide layer, which covers the monolayer graphene sheet on the sub-

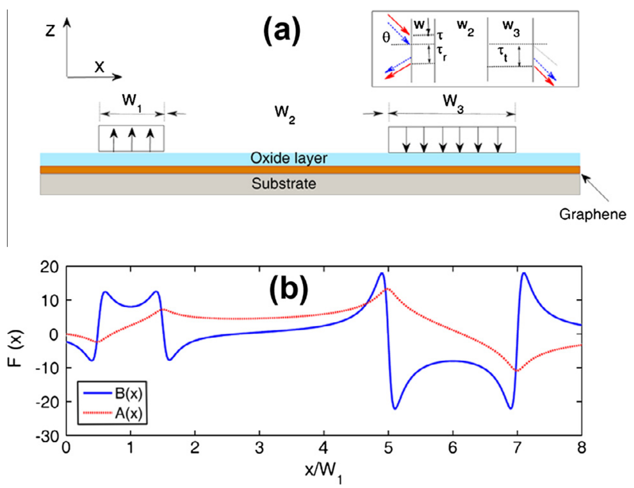

Fig. 1. (a) Schematic diagram of asymmetric graphene double magnetic barrier structure, where double ferromagnetic stripes with contrary magnetization directions are deposited on graphene separated by an insulated oxide layer. The inset denotes the lateral GH shifts of reflected (transmitted) upper (red solid line) and lower (blue dash line) components with a relative displacement τ. (b) Magnetic field **B** and corresponding vector potential **A** as functions of coordinate x with $F(x) = B(x)$ or $A(x)$. (For interpretation of the references to color in this figure legend, the reader is referred to the web version of this article).

strate. One ferromagnetic strip with magnetization direction perpendicular to graphene in x–z plane produces a magnetic field with its profile

$$B_0[K(x+W/2,\ z_0) - K(x-W/2,\ z_0)]\hat{z} \tag{1}$$

where W is the width of strip, z_0 is the distance of the field point to the strip and B_0 is a constant related to aspect ratio of the stripe, with $K(x,\ z_0) = \left(2Wx/x^2 + z_0^2\right)$ [44]. Therefore, we can similarly obtain the magnetic field $\mathbf{B}(\mathbf{r})$ induced by double ferromagnetic strips with contrary magnetization directions, and their widths W_1 and W_3, respectively, as shown in Fig. 1b (blue[1] solid line) with $z_0 = 0.1$. Using Landau gauge and $\mathbf{B}(\mathbf{r}) = \nabla \times \mathbf{A}(\mathbf{r})$, we can obtain the vector potential $\mathbf{A}(\mathbf{r}) = (0, A(x), 0)$ with $A(x) = \int_0^x B(x)dx$, as shown in Fig. 1b (red dash line).

In this graphene system, Dirac fermions obey the massless Dirac equation:

$$v_F\ \sigma\ \cdot\ [-i\hbar\nabla + e\mathbf{A}(\mathbf{r})]\psi(\mathbf{r}) = E\ \psi(\mathbf{r}) \tag{2}$$

where $\boldsymbol{\sigma} = (\boldsymbol{\sigma}_x, \boldsymbol{\sigma}_y)$ is 2D Pauli matrix vector, $\psi(\mathbf{r}) = [\psi_A(x), \psi_B(x)]^{\mathrm{T}}$ is the two-component pseudospinor. To simplify the notation, we can conveniently introduce dimensionless units: $L_B = \sqrt{\hbar/eB_0}$, $x \to L_B\, x$, $A(x) \to L_B B_0 A(x)$, $k_y \to 1/L_B k_y$, $E_0 = \hbar v_F/L_B$ and $E \to E_0 E$. At a typical value of $B_0 \approx 0.1$ T, the length and energy scales are $L_B \approx 80$ nm and $E_0 \approx 7$ meV, respectively. Due to the invariance of momentum along the y direction, the wavefunction can be written as $\psi(\mathbf{r}) = \psi(x)\exp(ik_y y)$ and Eq. (2) can be further reduced as:

$$\left[\partial_x^2 - (k_y + A(x))^2 \mp \partial_x A(x) + E^2\right]\psi_{A(B)}(x) = 0 \tag{3}$$

When a finite-sized incident Gaussian electron beam is considered, the wave functions of the incident, reflected and transmitted beams satisfying Eq. (3) can be assumed to be

$$\psi_{in}(x,y) = \int_{-\infty}^{\infty} dk_y\ u(k_y - \bar{k}_y)e^{ik_y y + ik_x(k_y)x}\begin{bmatrix} 1 \\ e^{i\theta(k_y)} \end{bmatrix} \tag{4.1}$$

$$\psi_r(x,y) = \int_{-\infty}^{\infty} dk_y\ r(k_y)\ u(k_y - \bar{k}_y)e^{ik_y y - ik_x(k_y)x}\begin{bmatrix} 1 \\ e^{i\theta(k_y)} \end{bmatrix} \tag{4.2}$$

$$\psi_t(x,y) = \int_{-\infty}^{\infty} dk_y\ t(k_y)\ u(k_y - \bar{k}_y)e^{ik_y y + A_f y + ik_x(k_y)x}\begin{bmatrix} 1 \\ \sqrt{k_x^i/k_x^f}e^{i\alpha(k_y)} \end{bmatrix} \tag{4.3}$$

where the Gaussian envelope is taken as $u(k_y - \bar{k}) = \exp\left(-(k_y - \bar{k})^2/2\Delta_k^2\right)$ so that the wavepacket is sharply peaked at $k_y = \bar{k}_y$, θ is the incident angle, α is the emergent angle, and $k_x^i = \sqrt{E^2 - k_y^2}$ and $k_x^f = \sqrt{E^2 - (k_y + A_f)^2}$ are corresponding longitude wave vectors in incident and emergent regions with A_f as the vector potential of emergent regions. The reflection coefficient $r(k_y) = |r(k_y)|\exp\left[i\mu_r(k_y)\right]$ and the transmission coefficient $t(k_y) = |t(k_y)|\exp\left[i\mu_t(k_y)\right]$ can be obtained by the transfer matrix method [5–11], with reflection phase $\mu_r(k_y)$ and transmission phase $\mu_t(k_y)$, respectively.

The stationary-phase approximation is widely applied to the GH shift calculations and shows that the GH shifts of reflected (transmitted) beam result from the negative gradient of the reflection (transmission) phase in direction [37–43]. For Dirac fermions in graphene-based structure, the upper and lower lateral shifts for the reflected and transmitted beams can be given by:

$$\tau_r^{\pm} = -d\mu_r/dk_y|_{\bar{k}_y} \mp \tau \tag{5.1}$$

$$\tau_t^{\pm} = -d\mu_t'/dk_y|_{\bar{k}_y} \tag{5.2}$$

[1] For interpretation of color in Fig. 1, the reader is referred to the web version of this article.

where $\mu_t' = \mu_t + \sum_{j=1}^{3} k_x^j W_j$ relates to the berry phase [31], and τ is the relative displacement between upper and lower components of the incident beam. Usually, the average shifts $\tau_{r,t} = \left(\tau_{r,t}^{+} + \tau_{r,t}^{-}\right)/2$ are used to denote the GH shifts.

3. Results and discussions

As long as the edge-smearing length of magnetic barrier is much smaller than the Fermi wavelength of quasiparticle in the structure, it can be well approximated as a rectangular barrier. Accordingly, in this section, we first consider asymmetric graphene double rectangular magnetic barrier structures and then further discuss the real magnetic structure described by Eq. (1).

Fig. 2 shows a few contour plots of transmission T ($T = |t|^2$) of electrons through asymmetric double rectangular magnetic barriers in graphene. The asymmetry of double magnetic barriers is mainly induced by their magnetization directions and widths. Some values of widths for the magnetic barriers with contrary magnetization $B_1 = 1$ and $B_3 = -1$ are used: $W_1 = W_2 = W_3 = 1$ in Fig. 2a; $W_1 = W_3 = 1$ and $W_2 = 2$ in Fig. 2b; $W_1 = 2$ and $W_2 = W_3 = 1$ in Fig. 2c; $W_1 = W_2 = 1$ and $W_3 = 2$ in Fig. 2d. It is clear that

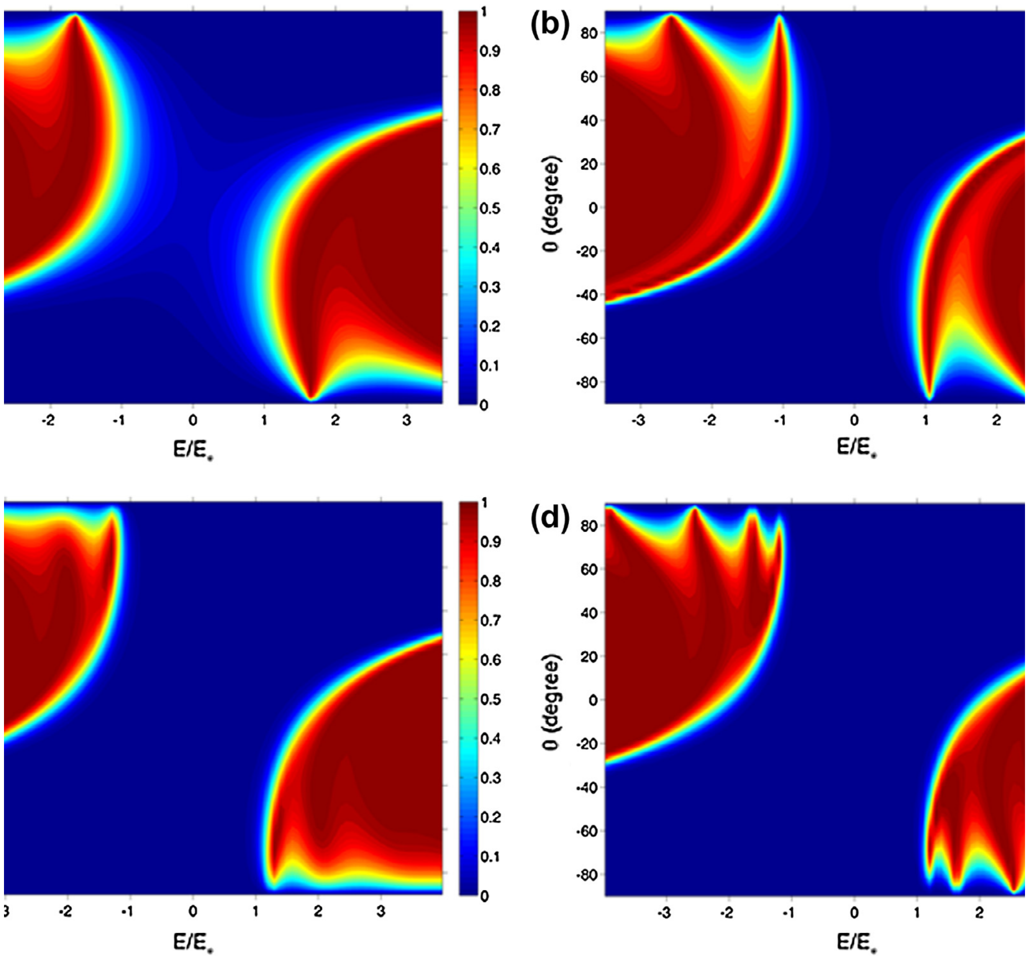

Fig. 2. Contour plot of the transmission as a function of energy E and incident angle θ for rectangular barriers. (a) $W_1 = W_2 = W_3 = 1$. (b) $W_1 = W_3 = 1$ and $W_2 = 2$. (c) $W_1 = 2$ and $W_2 = W_3 = 1$. (d) $W_1 = W_2 = 1$ and $W_3 = 2$.

the transmission exhibits unique behavior owing to the chiral nature of the electronic states in graphene. More importantly, a transmission gap occurs in all structures, depends on the incident angle and can be changed by widths of barriers and the distance between the double barriers. Magnetically induced transmission gap in graphene is previously supported in symmetric double or multi magnetic barriers, which can widen the gap by increasing the number of barriers [6]. In fact, this transmission gap arises from the magnetic confinement, which suppresses the Klein tunneling [5,6]. In this present work, double magnetic barriers with contrary magnetization directions also have the transmission gap and the tunability of gap can be achieved by the widths and distance of the double barriers. Thus, one can use the graphene magnetic structure to design a tunable electron wave filter. In addition, the magnetic structure can be used to laterally manipulate the reflected and transmitted electrons or holes by the lateral GH shift at the interfaces between the barrier and well.

In order to further evaluate the effect of the incident angle on the transmission gap and the GH shift, we calculated the transmission and GH shift as functions of Fermi energy at some different incident angles and plot them in Fig. 3. It is clearly observed that the width ΔE of transmission gap is enhanced with increasing the incident angle and electrons or holes exhibit obvious GH shift at the edge of gap. The larger the incident angle is, the stronger magnetic confinement for carriers becomes, and hence the gap and GH shift increase.

Fig. 4 shows the transmission and GH shift as functions of Fermi energy at some specific distances w_2. It can be clearly seen that the transmission gap becomes deeper and the GH shifts are enhanced with increasing the distance between the two barriers. Since the vector potential induced by the two magnetic barriers with contrary magnetization directions can be equivalent to an effective potential, which can confine electrons or holes, the wavevector becomes imaginary and in turn leads to the transmission probability damping exponentially for the distance w_2. Therefore, the gap becomes deeper with increasing w_2. The effective potential is also supported by double δ magnetic barriers used as electron waveguide [17,22–24]. In this present work, we pay attention to the transmission gap and the GH shift. The tunability of the gap and GH shift depending on the distance of two barriers indicates that the structure can be well proposed to filter and manipulate electron wave in graphene.

To evaluate the transmission and GH shift in real asymmetric graphene double magnetic barrier structures, we numerically calculate the transmission and GH shift at some specific thickness z_0 of oxide layer and plot the results in Fig. 5. As can be seen, not only the transmission gap and GH shift remain, but also they can be tuned by the thickness of oxide layer. Compared with the rectangular barrier, the width of the transmission gap becomes narrow, but the smoothness of the real magnetic barriers will not restrict the use of the electron wave filter. On the contrary, one can use the real magnetic

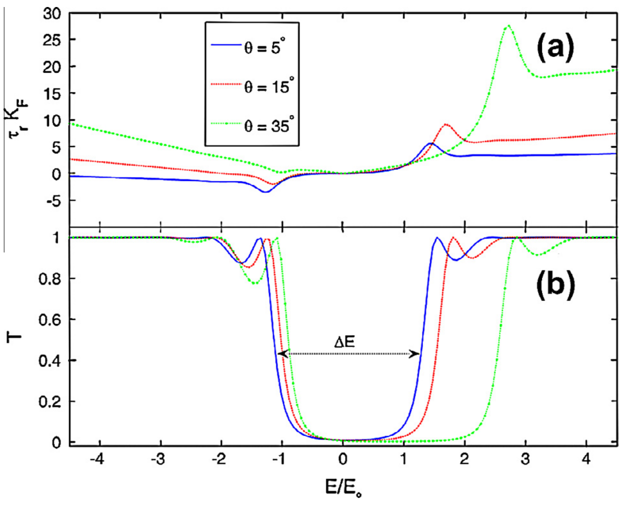

Fig. 3. The transmission as a function of energy E at some specific angles (b). Corresponding GH shifts (a). The physical parameters for square barriers are $W_1 = W_3 = 1$ and $W_2 = 2$.

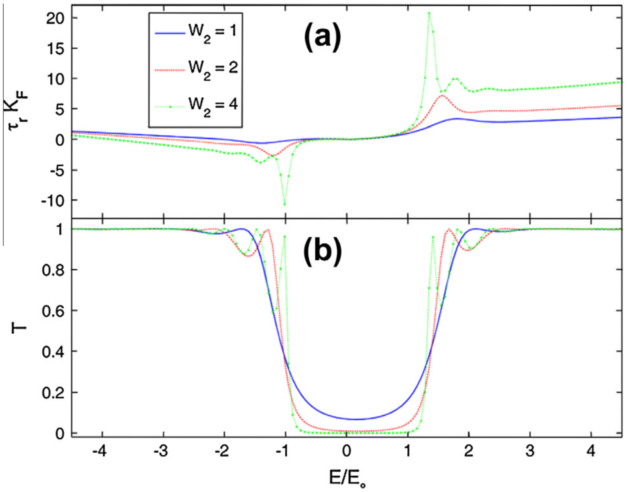

Fig. 4. The transmission as a function of energy E at some specific distance between the double barriers (b). Corresponding GH shifts (a). The physical parameters for square barriers are $W_1 = W_3 = 1$ and $\theta = 15°$.

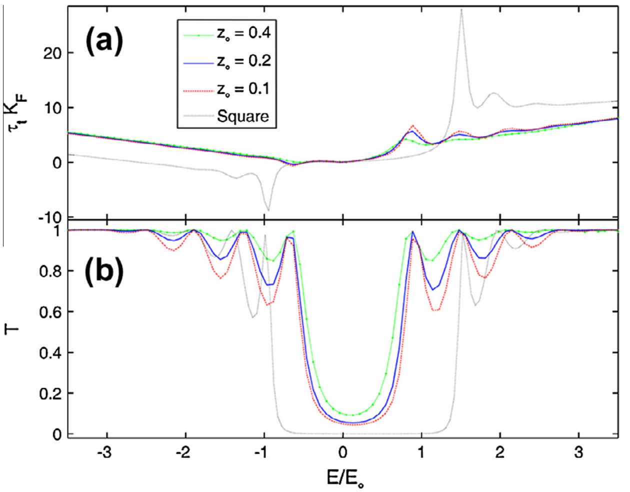

Fig. 5. The transmission as a function of energy E at some specific thickness of oxide layer (b). Corresponding GH shifts (a). The physical parameters for real magnetic barrier $W_1 = W_3 = 1.5$, $W_2 = 2$, $B_0 = 0.1$ T and $\theta = 15°$.

barriers induced by ferromagnetic strip to filter the electron wave by the transmission gap. Furthermore, the real magnetic barriers can be applied to manipulate Dirac fermions in graphene by the GH shift.

Finally, it should be mentioned that the Zeeman interaction leading to spin filter and spin-dependent GH shift has been investigated in two-dimensional electron gas under strong magnetic field [45,46]. In this present work, the Zeeman interaction under weak magnetic field is very small in graphene so that all spin effects can be neglected, which is supported in previous investigations [5–12]. Similarly, one can also discuss the spin-dependent filter and GH shifts in asymmetric graphene DMBs, if the strong magnetic field is considered.

4. Conclusion

In summary, we have investigated the transmission and the quantum GH shifts in asymmetric graphene double magnetic barrier structure. The main outcomes of the work are formulated as follow:

(1) A transmission gap occurs in asymmetric graphene DMBs and arises from the magnetic confinements.
(2) The width of the transmission gap is dependent on the incident angle and can be tuned by the barrier's width and the distance between the double barriers.
(3) The real magnetic barriers induced by ferromagnetic strips not only remain the transmission gap but also increase the tunability of gap by changing the thickness of insulated oxide layer.
(4) Electrons or holes exhibit obvious GH shift at the edge of the transmission gap and the GH shift are tuned by the incident angle as well as the physical structure of graphene DMBs.

The tunable transmission gap and quantum GH shift in the asymmetric graphene DMBs may lead to possible application in tunable electron wave filter and lateral manipulation of Dirac fermions in graphene. The quantum GH shift also demonstrates electronic analogies of optical behaviors in micro-structure and potential application in manipulation of low-dimensional electron gas [47,48].

Acknowledgements

This work was supported by the NSFC (Nos. 10902128, 10732100 and 11072271) and Specialized Research Fund for the Doctoral Program of Higher Education of China (No. 20120171110005).

References

[1] K.S. Novoselov, A.K. Geim, S.V. Morozov, D. Jiang, Y. Zhang, S.V. Dubonos, I.V. Grigorieva, A.A. Firsov, Science 306 (2004) 666–669.
[2] K.S. Novoselov, A.K. Geim, S.V. Morozov, D. Jiang, M.I. Katsnelson, I.V. Grigorieva, S.V. Dubonos, A.A. Firsov, Nature 438 (2005) 197–200.
[3] Y. Zhang, Y.W. Tan, H.L. Stromer, P. Kim, Nature 438 (2005) 201–204.
[4] V.M. Apalkov, T. Chakraborty, Phys. Rev. Lett. 97 (2006) 126801.
[5] A. De Martino, L. Dell'Anna, R. Egger, Phys. Rev. Lett. 98 (2007) 066802;
A. De Martino, L. Dell'Anna, R. Egger, Solid State Commun. 144 (2007) 547–550.
[6] M. Ramezani Masir, P. Vasilopoulos, F.M. Peeters, Appl. Phys. Lett. 93 (2008) 242103.
[7] M. Ramezani Masir, P. Vasilopoulos, A. Matulis, F.M. Peeters, Phys. Rev. B 77 (2008) 235443.
[8] M. Ramezani Masir, P. Vasilopoulos, F.M. Peeters, New J. Phys. 11 (2009) 095009.
[9] S. Ghosh, M. Sharma, J. Phys. Condens. Matter 21 (2009) 292204.
[10] L. Dell'Anna, A. De Martino, Phys. Rev. B 79 (2009) 045420;
L. Dell'Anna, A. De Martino, Phys. Rev. B 83 (2011) 155449.
[11] L. Sun, C. Fang, Y. Song, Y. Guo, J. Phys.: Condens. Matter 22 (2010) 445303.
[12] L.Z. Tan, C.-H. Park, S.G. Louie, Phys. Rev. B 81 (2010) 195426.
[13] H. Xu, T. Heinzel, M. Evaldsson, S. Ihnatsenka, I.V. Zozoulenko, Phys. Rev. B 75 (2007) 205301.
[14] S. Park, H.S. Sim, Phys. Rev. B 77 (2008) 075433.
[15] A. Kormányos, P. Rakyta, L. Oroszlány, J. Cserti, Phys. Rev. B 78 (2008) 045430.
[16] L. Oroszlány, P. Rakyta, A. Kormányos, C.J. Lambert, J. Cserti, Phys. Rev. B 77 (2008) 081403(R).
[17] T.K. Ghosh, A. De Martino, W. Häusler, L. Dell'Anna, R. Egger, Phys. Rev. B 77 (2008) 081404(R).
[18] M. Ramezani Masir, P. Vasilopoulos, F.M. Peeters, J. Phys.: Condens. Matter 23 (2011) 315301.
[19] Y.P. Bliokh, V. Freilikher, F. Nori, Phys. Rev. B 81 (2010) 075410.
[20] D. Wang, G. Jin, Europhys. Lett. 88 (2009) 17011.
[21] W. Häusler, A. De Martino, T.K. Ghosh, R. Egger, Phys. Rev. B 78 (2008) 165402.
[22] N. Myoung, G. Ihm, Physica E 42 (2009) 70–72.
[23] N. Myoung, G. Ihm, S.J. Lee, Phys. Rev. B 83 (2011) 113407.
[24] W. Huang, Y. He, Y. Yang, C. Li, J. Appl. Phys. 111 (2012) 053712.
[25] F. Zhai, K. Chang, Phys. Rev. B 77 (2008) 113409.
[26] B. Soodchomshom, I.M. Tang, R. Hoonsawat, Physica E 41 (2009) 1310–1314.
[27] F. Zhai, X. Zhao, Kai Chang, H.Q. Xu, Phys. Rev. B 82 (2010) 115442.
[28] M. Tahir, K. Sabeeh, Phys. Rev. B 77 (2008) 195421.
[29] R. Nasir, K. Sabeeh, M. Tahir, Phys. Rev. B 81 (2010) 085402.
[30] H. Xu, T. Heinzel, M. Evaldsson, I.V. Zozoulenko, Phys. Rev. B 77 (2008) 245401.
[31] A.V. Shytov, M.S. Rudner, L.S. Levitov, Phys. Rev. Lett. 101 (2008) 156804.
[32] M. Ramezani Masir, P. Vasilopoulos, F.M. Peeters, Phys. Rev. B 82 (2010) 115417.

[33] V.M. Pereira, A.H. Castro Neto, Phys. Rev. Lett. 103 (2009) 046801.
[34] X. Chen, J.-W. Tao, Appl. Phys. Lett. 94 (2009) 262102.
[35] M.I. Katsnelson, K.S. Novoselov, A.K. Geim, Nat. Phys. 2 (2006) 620–625.
[36] F. Goos, H. Hänchen, Ann. Phys. 436 (1947) 333;
F. Goos, H. Hänchen, Ann. Phys. 440 (1949) 251.
[37] C.W.J. Beenakker, R.A. Sepkhanov, A.R. Akhmerov, J. Tworzydło, Phys. Rev. Lett. 102 (2009) 146804.
[38] M. Sharma, S. Ghosh, J. Phys.: Condens. Matter 23 (2011) 055501.
[39] Z. Wu, F. Zhai, F.M. Peeters, H.Q. Xu, K. Chang, Phys. Rev. Lett. 106 (2011) 176802.
[40] F. Zhai, Y. Ma, K. Chang, New J. Phys. 13 (2011) 083029.
[41] X. Chen, J.-W. Tao, Y. Ban, Eur. Phys. J. B 79 (2011) 203–208.
[42] Y. Song, H.-C. Wu, Y. Guo, Appl. Phys. Lett. 100 (2012) 253116.
[43] Y. Wang, Y. Liu, B. Wang, http://dx.doi.org/10.1016/j.physe.2013.01.008.
[44] A. Matulis, F.M. Peeters, P. Vasilopoulos, Phys. Rev. Lett. 72 (1994) 1518.
[45] X. Chen, X.J. Lu, Y. Wang, C.F. Li, Phys. Rev. B 83 (2011) 195409.
[46] L. Dell'Anna, A. De Martino, Phys. Rev. B 80 (2009) 155416.
[47] S. Datta, Electronic Transport in Mesoscopic Systems, Cambridge University Press, New York, 1995. pp. 276–290.
[48] D. Dragoman, M. Dragoman, Quantum–Classical Analogies, Springer, Berlin, 2004.